

# Simple mathematical model for predicting the transient behaviour of an ice-bank system

S. I. Finer and A. C. Cleland

Department of Process and Environmental Technology, Massey University, Palmerston North, New Zealand

S. J. Lovatt

Meat Industry Research Institute of New Zealand, PO Box 617, Hamilton, New Zealand

Received 31 December 1991; revised 16 June 1992

The time-variable performance of a Refrigerant 22 ice-bank system was simulated by a dynamic model which was derived by assuming that heat transfer was always the limiting process, and which thus ignored hydrodynamic processes. The model comprised four ordinary differential equations describing the position of the ice front, the water temperature, and the refrigerant evaporation and condensation temperatures, each of which was derived by energy balance, plus a number of algebraic equations. Measured plant performance was accurately predicted except immediately after start-up, and in circumstances in which the assumption that the dynamics of refrigerant flow did not exert any controlling influence on the overall process dynamics was inadequate (for example, when the thermostatic expansion valve operation becomes unstable). The model requires only data that should be readily available or can be easily estimated, and thus it is suitable for analyses in the design of ice bank systems to handle time-varying conditions. Simple dynamic models ignoring hydrodynamics can be adequate in circumstances where the main source of variation arises beyond the refrigeration circuit itself.

(Keywords: ice bank; dynamics; modelling)

## Modèle mathématique simple pour prévoir le comportement transitoire d'un bac à glace

*On a simulé la performance variable avec le temps d'un bac à glace au R22 avec un modèle dynamique que l'on a obtenu en supposant que le transfert de chaleur était toujours le processus limitant et, ainsi, en ignorant les processus hydrodynamiques. Le modèle se composait de quatre équations différentielles ordinaires décrivant la position du front de glace, la température de l'eau, les températures d'évaporation et de condensation du frigorigène; ces équations ont été obtenues par un bilan énergétique et par plusieurs équations algébriques. On a prévu avec précision la performance mesurée de l'installation, sauf immédiatement après la mise en marche, et dans le cas où la supposition selon laquelle la dynamique de l'écoulement du frigorigène n'exerce aucune influence sur la dynamique du processus complet était inadéquate (par exemple lorsque le fonctionnement du détendeur thermostatique est devenu instable). Le modèle exige des données qui soient immédiatement disponibles ou qui puissent être facilement évaluées; aussi convient-il pour les analyses de la conception des bacs à glace dans le but de définir les conditions variant avec le temps. Des modèles dynamiques simples ne tenant pas compte de l'hydrodynamique peuvent convenir dans des cas où la principale source de variation se produit au-delà du circuit frigorifique lui-même.*

(Mots clés: bac à glace; dynamique; modélisation)

Dynamic models of refrigeration systems are becoming increasingly common. Both model complexity and types of application for models vary enormously. There are detailed models of components such as compressors and valves in which transients that occur in a fraction of a second are being studied, there are models for predicting system start-up, and there are models for systems in which the normal operation occurs under transient rather than steady state conditions. Models for this latter group of applications normally simulate behaviour occurring over some minutes or even hours. They have been reviewed recently<sup>1</sup>, and a key question posed in this review was 'what is the appropriate level of model complexity for different applications of modelling?' It was contended that in many applications, and especially those in which the refrigeration end-user subjects the system to a time-variable heat load, simple models may be adequate. The basis of this hypothesis is that in such

applications heat transfer can be considered as the limiting factor. If the rate of heat release by the refrigeration user changes relatively slowly with time the refrigeration system, which is inherently faster acting (i.e. has a shorter time constant), will react in a manner that can be adequately described by energy balance considerations. This effectively implies that hydrodynamic aspects of refrigeration system performance are not limiting. For example, in a model of an evaporator it is assumed that there is always the same degree of wetting of the heat transfer surface even though this is known not to be true immediately after start-up.

Darrow *et al.*<sup>2</sup> used this approach (often referred to as 'thermal modelling') to model the transient behaviour of a simple refrigeration system cooling a tank of water from 20°C to 0°C. Their results showed that other than immediately after start-up transient behaviour of the water temperature, refrigeration condensation tempera-

**Nomenclature**

$A$	Surface area of ice ( $\text{m}^2$ )
$c$	Specific heat capacity ( $\text{J kg}^{-1} \text{K}^{-1}$ )
$f$	Unspecified functional relationship
$h$	Enthalpy ( $\text{J kg}^{-1}$ )
$k$	Thermal conductivity ( $\text{W m}^{-1} \text{K}^{-1}$ )
$L$	Length of cylindrical evaporator coil (m)
$m$	Mass flow rate ( $\text{kg s}^{-1}$ )
$M$	Mass (kg)
$(Mc)$	Thermal capacity ( $\text{J K}^{-1}$ )
$PR$	Pressure ratio
$P$	Pressure (Pa)
$Q$	Swept volume ( $\text{m}^3 \text{s}^{-1}$ )
$r$	Radius of evaporator tube (m)
$s$	Refrigerant superheat at evaporator outlet ( $^{\circ}\text{C}$ )
$t$	Time (s)
$(UA)$	Product of overall heat transfer coefficient and heat transfer area ( $\text{W K}^{-1}$ )
$v$	Specific volume of vapour at suction condition ( $\text{m}^3 \text{kg}^{-1}$ )

**Greek**

$\alpha$	Convection heat transfer coefficient ( $\text{W m}^{-2} \text{K}^{-1}$ )
----------	--

$\eta$	Compressor efficiency
$\theta$	Temperature ( $^{\circ}\text{C}$ )
$\rho$	Density ( $\text{kg m}^{-3}$ )
$\phi$	Heat gain from environment (W)

**Subscripts**

b	Tube wall
c	Condensation/condenser
cp	Compressor/compression (isentropic)
d	Discharge/discharge line
e	Evaporation
f	Ice
i	Inlet
o	Outlet
r	Refrigerant
s	Suction/suction line
t	Total water (liquid + solid)
v	Volumetric
w	Water existing as a liquid
y	Isentropic
1	Refrigerant/tube wall interface
2	Tube wall/ice interface
3	Ice front/water interface

ture and evaporation temperature was adequately modelled using only three ordinary differential equations (ODE). These differential equations were derived by energy balances around 'zones' assumed to be well-mixed and hence internally isothermal. The three zones were the water, the refrigerant side of the evaporator and the refrigerant side of the condenser. Darrow *et al.* concluded that good prediction was reliant on the major source of the variation (the variable heat load that arose from chilling of the water) being outside the refrigeration circuit itself, and that in other applications where this is not true such simple models may not be adequate. As well as reduced computational effort, the use of a single zone to represent each of the condenser and the evaporator has other advantages over more complicated models (e.g. those reviewed by Cleland<sup>1</sup> and James *et al.*<sup>3</sup>) such as substantially reduced data requirements.

In this paper an extension to the work of Darrow *et al.*<sup>2</sup> is reported. Ice-bank systems are being increasingly used in food industry applications where there is significant, but time-variable demand for chilled water production. The ice bank allows 'cold' to be stored at off-peak periods, and thus the refrigeration system can be sized for the 24 hour average load rather than the peak chiller demand. Additional advantages can be achieved by slightly oversizing the ice bank so that the system need not run at all when energy charges are high, allowing the operator to take advantage of cheaper night rates for energy supply. A disadvantage of the ice bank system compared to a chilled water system is that lower evaporation temperatures must be used, which lowers coefficient of performance, thus increasing energy use per unit refrigeration effect. This partially offsets the benefit of being able to use lower cost energy. An important consideration is just how much the evaporation temperature must be lowered. As ice builds up the effective heat

transfer coefficient between the ice/water surface and the refrigerant drops due to the increasing length of the heat conduction pathway in the ice, and this in turn leads to a dropping evaporation temperature if the compressor is not modulated. As the heat load changes the ice will partially melt and rebuild, so the mean evaporation temperature is not easily predicted. It would therefore be advantageous to be able to predict transient ice-bank performance during system design so that the true energy consumption rate under variable evaporation temperature conditions can be accurately estimated.

The objectives of this paper were therefore: (1) to provide further testing (beyond that of Darrow *et al.*<sup>2</sup>) of the hypothesis that simple 'thermal' dynamic models which treat heat exchangers as single zones can be adequate in applications where the source of the variation arises in the refrigeration user; and (2) to develop a dynamic model of an ice bank system that was simple yet accurate so that it could be used in ice-bank optimization. An important consideration was that if such a model was to be used at the design stage for an ice bank a minimum of data would be available.

**Theory**

Whilst the objective was to develop a generally applicable model for an ice bank, specific data for the model were chosen with reference to the experimental plant used. This plant is shown in *Figure 1*, and was largely the same plant as used by Darrow *et al.*<sup>2</sup> Since the work of Darrow *et al.* some plant modifications had been carried out which affected only vapour pipelines, but not the major plant components used in the present work.

The dynamic model was based on that of Darrow *et al.*<sup>2</sup>, but was extended to include the ice formation. In this respect the model development closely mirrored that

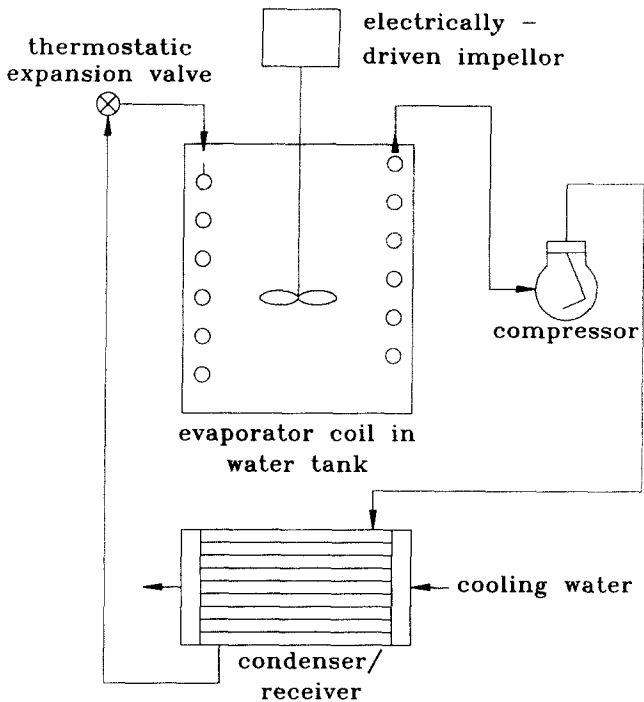


**Figure 1** Schematic diagram of experimental plant used in the study (not to scale). Only main plant items are shown. Equipment specifications are given by Darrow *et al.*  
 Figure 1 Schéma de l'installation expérimentale utilisée dans l'étude (non à l'échelle). Seuls les principaux composants sont présentés. Les spécifications sont données par Darrow *et al.*

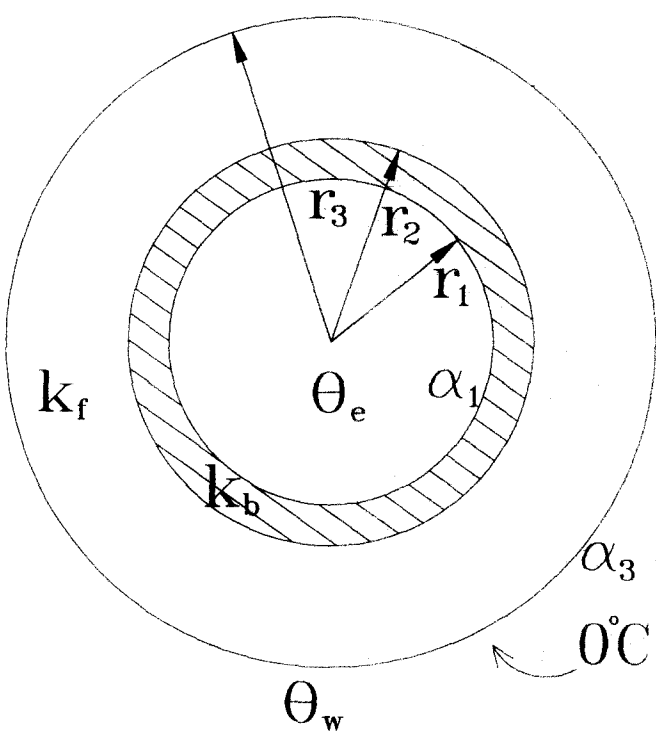


**Figure 2** Conceptual model and nomenclature for building of cylindrical ice on a smooth evaporator tube with internal radius  $r_1$  and external radius  $r_2$   
 Figure 2 Modèle conceptuel et nomenclature pour construire de la glace cylindrique sur un tube d'évaporateur lisse avec un rayon interne  $r_1$  et un rayon externe  $r_2$

outlined by Cleland<sup>1</sup> (pp 185–190). The model consists of two parts; the first when no ice is present, and the second when ice exists. There is also a need for a criterion to transition between the two model parts. The model of Darrow *et al.*<sup>2</sup> is as follows:

In the absence of ice ( $M_f = 0$ ):

$$(Mc)_c \frac{d\theta_c}{dt} = -(UA)_c \Delta\theta_c + m_r(h_{ci} - h_{co}) - \phi_c \tag{1}$$

$$(Mc)_e \frac{d\theta_e}{dt} = (UA)_e (\theta_w - \theta_e) + m_r(h_{ei} - h_{eo}) \tag{2}$$

$$(Mc)_w \frac{d\theta_w}{dt} = (UA)_e (\theta_e - \theta_w) \tag{3}$$

$$m_r = Q_{cp} \frac{\eta_v}{v} \tag{4}$$

$$h_{ci} = h_{cpi} + \frac{\Delta h_{cp}}{\eta_y} + \frac{\phi_{cp}}{m_r} \tag{5}$$

$$P_e = f(\theta_e) \tag{6}$$

$$P_s = P_e - \Delta P_s \tag{7}$$

$$P_c = f(\theta_c) \tag{8}$$

$$P_d = P_c + \Delta P_d \tag{9}$$

$$v = f(P_s, \theta_e, s) \tag{10}$$

$$h_{cpi} = h_{co} + \frac{\phi_s}{m_r} \tag{11}$$

Expressed in this fashion, the model is general and applies to equipment configurations other than that in Figure 1.

The expected temperature profile through each circuit in the evaporator is a gradually changing evaporation temperature (due to changes in both static head effects and pipeline pressure drop) followed by a dry section in which the gas superheats. In the above model this complex situation is represented by a single evaporation temperature, and it is assumed that Equations (2) and (3) adequately describe the heat transfer. Using thermodynamic data for the refrigerant, the evaporator exit enthalpy ( $h_{eo}$ ) is calculated from the evaporation temperature ( $\theta_e$ ), evaporator pressure ( $P_e$ ) and refrigerant exit superheat ( $s$ ). The effect of the superheating of the vapour in the dry section of the evaporator is thus directly included. The value of  $s$  used was the mean measured value across all trials. To determine the condenser outlet enthalpy ( $h_{co}$ ) it was assumed that the liquid refrigerant left the condenser saturated.

Once ice-building commences this is assumed to be outwards cylindrical growth on the bare copper tube. Figure 2 illustrates the situation. It is necessary to replace Equations (2) and (3) by the following equations.

#### Water tank

In the situation with ice present, the model for the water system has two changes; first, the mass of water is changing, and second, the heat transfer is now started in terms of transfer to the ice/water interface at 0°C. Thus in Equation (3) the term  $(Mc)_w$  can no longer be used and the replacement equations are:

In the presence of ice ( $M_f > 0$ ):

$$c_w \frac{d(M_w \theta_w)}{dt} = \alpha_3 A_3 (\theta_w - 0) \quad (12)$$

$$\theta_w = (M_w \theta_w) / M_w \quad (13)$$

$$M_w = M_t - M_f \quad (14)$$

$$A_3 = 2\pi r_3 L \quad (15)$$

#### Ice front

In modelling the release of heat at the ice front it is assumed that the latent heat effects are dominant, i.e. when a water molecule leaves the bulk water and joins the solid phase the heat extraction required is the latent heat of freezing ( $\Delta h_{fw}$ ), but the sensible heat component ( $c_w \theta_w$ ) is ignored. Further, it is assumed that the ice already present offers heat transfer resistance, but no thermal capacity, i.e. any heat in cooling it below  $0^\circ\text{C}$ , and towards  $\theta_c$  is ignored (in practice there will be a temperature gradient from  $0^\circ\text{C}$  at the water interface to the tube wall temperature at the tube interface). These assumptions are the well-known 'steady-state' assumptions of Plank<sup>4</sup>. Once these assumptions are made the energy balance becomes:

In the presence of ice ( $M_f > 0$ ):

$$\Delta h_{fw} \frac{dM_f}{dt} = (UA)_f (0 - \theta_c) - \alpha_3 A_3 (\theta_w - 0) \quad (16)$$

$$\frac{1}{UA_f} = \frac{1}{2\pi L} \left[ \frac{1}{\alpha_1 r_1} + \frac{\ln(r_2/r_1)}{k_b} + \frac{\ln(r_3/r_2)}{k_f} \right] \quad (17)$$

$$r_3 = \left( \frac{M_f / \rho_f + \pi r_2^2 L}{\pi L} \right)^{1/2} \quad (18)$$

Approximations that could be used to improve the energy balance would be to replace  $\Delta h_{fw}$  by  $(\Delta h_{fw} + c_w \theta_w)$  or by  $(\Delta h_{fw} + c_w \theta_w - 0.5c_f \theta_c)$ . In the latter case, the last term is based on the assumption that on average the ice forming will eventually cool to a temperature halfway between the evaporation temperature and  $0^\circ\text{C}$ .

#### Evaporation temperatures

Equation (2) is replaced by:

In the presence of ice ( $M_f > 0$ ):

$$(Mc)_e \frac{d\theta_e}{dt} = (UA)_f (0 - \theta_c) + m_r(h_{ei} - h_{eo}) \quad (19)$$

#### Criterion for transition

When no ice is present ( $M_f = 0$ ) the criterion for ice formation to start is for the right hand side of Equation (16) with  $r_3$  set equal to  $r_2$  to be positive. Once this situation is reached then Equations (2) and (3) are replaced by Equations (12) to (19) with the initial condition  $M_f = 0$ . Conversely, when ice is melting, once the calculated value of  $r_3$  is less than or equal to  $r_2$  then the calculation transfers back to Equations (2) and (3), and the right hand side of Equation (16) is again checked.

In terms of implementation of these criteria, in a numerical integration procedure a potential problem that can arise is that the transitions are required to occur part way through a time step. The simplest procedure is to accept some error, and in the case of transition to ice formation keep  $M_f$  set to zero until the end of the time step in which ice formation restarts, or in the reverse case to arbitrarily set  $r_3$  equal to  $r_2$  for the remainder of the time step but still use Equations (12) to (19) otherwise. Less error can be achieved if the time step is reduced once it is sensed that the switchover will soon occur. Thus, the length of time for which an arbitrary assumption is applied is minimized. However, greatest accuracy is possibly by an iterative search seeking a shortened time step length that will make the time step end at exactly the time of transition between models.

#### Experimental

Experimental data collection was of two types – input data required to use Equations (1) to (19), and measured data for the transient performance of the ice-bank system.

#### Input data for the model

Because the work was an extension of earlier work by Darrow *et al.*<sup>2</sup>, many data used in the earlier study could still be applied. Data transferred through from this earlier study included  $(Mc)_e$ ,  $(Mc)_f$ ,  $(UA)_e$ ,  $(UA)_f$ ,  $\eta_v$ ,  $\eta_y$ ,  $s$  and  $Q_{cp}$ . Data that were physically measured were dimensions such as  $r_1$ ,  $r_2$  and  $L$ . Data obtained from thermodynamic and transport data compilations included  $\Delta h_{fw}$ ,  $c_w$ ,  $c_f$ ,  $k_b$ ,  $k_f$  and  $\rho_f$ . Each of these was assumed to be independent of temperature. The polynomial curve-fits of Cleland<sup>5</sup> that have been proven to be an accurate, yet computationally efficient means of calculating refrigerant thermodynamic properties were employed.

The overall  $(UA)_e$  value for the evaporator had been measured by Darrow *et al.*<sup>2</sup> as  $1166 \text{ W K}^{-1}$ , but in the second stage of the modelling it was also necessary to separate this value into separate estimates of  $\alpha_1$  and  $\alpha_3$ . The latter film coefficient is the film coefficient for convection between a well-stirred tank of water and an internal coil, a situation for which a number of dimensionless correlations are available. The best estimate of  $\alpha_3$  thus obtained was  $2300 \text{ W m}^{-2} \text{ K}^{-1}$ , and  $\alpha_1$  was estimated by back-calculation from  $(UA)_e$  as  $430 \text{ W m}^{-2} \text{ K}^{-1}$ .

#### Measurements of transient behaviour

In theory the model should apply to any ice bank subjected to a time-varying heat load. The equipment available precluded testing other than pull-down curves in which the tank of water cooled, and then ice formation occurred. Nevertheless, if the model adequately explains this behaviour it should be adequate for other heat load regimes.

A test run consisted of filling the tank shown in Figure 1 with water at about  $20\text{--}25^\circ\text{C}$ , turning on the impeller, and then the refrigeration. Cooling was continued for periods of 1 to 2 hours, at which point substantial ice growth had occurred. During this time readings were taken at one minute intervals as follows:

- compressor suction pressure
- compressor discharge pressure
- pressure at condenser entry
- pressure at evaporator exit
- water temperature
- refrigerant mass flow rate
- water height in the tank
- miscellaneous temperatures around the refrigeration circuit.

Pressures were measured in gauges rated as accurate to  $\pm 10$  kPa. The gauge set was checked internally for consistency, and differences between gauges were less than 20 kPa at conditions that could occur during the transient runs. Water temperature was read using four thermocouples calibrated to  $\pm 0.25^\circ\text{C}$ , and other temperatures by semi-conductor probes rated to better than  $\pm 1^\circ\text{C}$ . Refrigerant mass flow rate was measured by a turbine flow meter. This meter had been calibrated by a number of steady state trials in which the mass flow rate through the system was back-calculated from the water cooling achieved in a separate shell and tube evaporator. The expected accuracy was within  $\pm 10\%$ . Water height was used as a measure of the amount of ice formed. Because ice formation did not commence until the water temperature was close to  $0^\circ\text{C}$ , changes in water density were negligibly small, so any increase in water height could be attributed to ice formation. An inclined tube was built to increase sensitivity of measurement. Some difficulties were experienced with variations in liquid height due to the action of the tank impeller, and to surface tension effects when ice formation was very slow, but once the ice formation was significant the effect of these error sources reduced. The mass of ice was calculated from the volume change.

There were some difficulties due to loss of refrigerant. A slow leak of refrigerant had been occurring during the time of the work, and this had been hard to trace. It was eventually found in a system component not used in the present work, but a result of the problem was that each test run was conducted with a different refrigerant charge to the other runs. Three runs in which there was sufficient charge that there was no indication of vapour presence in the liquid line sight glass were performed. These gave the same general trends when comparisons between experimental and predicted data were made, but the varying charge may have had some effect as will be seen.

To make easy comparisons with the predicted data the suction and discharge pressures were converted to equivalent saturation temperatures – saturated suction temperature and saturated discharge temperature. The measured refrigerant mass flow rate, the water temperature, and the calculated ice accumulation could be compared directly to the simulated results.

## Results

The model described by Equations (1) to (9) was numerically integrated by a continuous system modelling package using a fifth order method based on the well-known fourth order Runge–Kutta procedure. There was error control on the time step so that numerical integration errors could be kept negligibly small, and it was observed that the time step adjuster handled the model transition adequately by moving to very small time steps at the time

of transition. For each run measured data were used to establish initial conditions for each of the dynamic variables. Nevertheless, in the implementation of the model a number of decisions had to be made.

Like Darrow *et al.*<sup>2</sup>, it was decided to ignore heat losses from condenser, pipework and compressor (i.e.  $\phi_c$ ,  $\phi_{cp}$ , and  $\phi_s$  were assumed to be zero). Whereas Darrow *et al.* had assumed pipeline pressure drops to be negligible, this assumption was no longer considered valid. Modifications to the plant between the two studies had led to the installation of a number of new bends and valves, plus longer lengths of straight pipe, so it was considered necessary to include pressure drop allowances.

Two approaches could be employed to estimate pressure drop; an experimental approach in which measured data were regressed against flow rate to achieve a line of best fit, or a theoretical analysis of the pipeline behaviour. The first approach has the disadvantage that large amounts of data for differing conditions can only be effectively collected during dynamic runs, which reduces the independence of the estimate of pressure drop from the dynamic test data. The latter relies on the effects of bend and valves being accurately determined. The disadvantage of this procedure was that none of the straight line sections of the pipe was very long, and so end effects on each pipe could be significant, thus making it hard to achieve good theoretical estimates. It was decided to use the regression, but to cross-check by the theoretical approach.

Fluid dynamics theory suggests that in well-developed turbulent flow, and across small working ranges pressure drop is proportional to the product of fluid density and velocity squared. By elementary algebra this dependency can be re-expressed as pressure drop being proportional to the square of mass flow rate, and the reciprocal of vapour density. In the present situation for the particular pipelines involved, the pressure drop is primarily affected by the change in mass flow rate. Therefore, a regression line relating measured pressure drop to the square of mass flow rate was fitted to all available data, and cross-checks made using theoretical estimates. These generally agreed within  $\pm 20\%$  of both the regression line and measured pressure drops for each run.

Figures 3, 4 and 5 show predicted and measured temperatures for each of the three runs. Figures 6, 7 and 8, the predicted and measured refrigerant mass flow rate, and Figures 9, 10 and 11, the predicted and measured ice masses. In the latter three figures, it is seen that the shape of the ice formation lines agrees well until about 75 kg of ice are present, and then starts to diverge. The reason for the slowing of the experimental ice formation rate is that once the ice thickness built up to about 75 kg the ice fronts from adjacent evaporator tubes met and joined, thus reducing the area available for new ice formation. Therefore, in interpreting the results for Runs 2 and 3, only the data for times up to about 5000 s can be considered valid. No such problem arose for Run 1.

The main area of disagreement on Figures 9, 10 and 11 is in the time that ice first starts to form, which then leads to offset of the measured from the predicted lines. As already mentioned, some difficulties were experienced in getting reliable experimental data at short times, but the major reason probably lies elsewhere. One possibility is that heat transfer across the evaporator as a whole is not homogeneous as assumed in the model. There would be

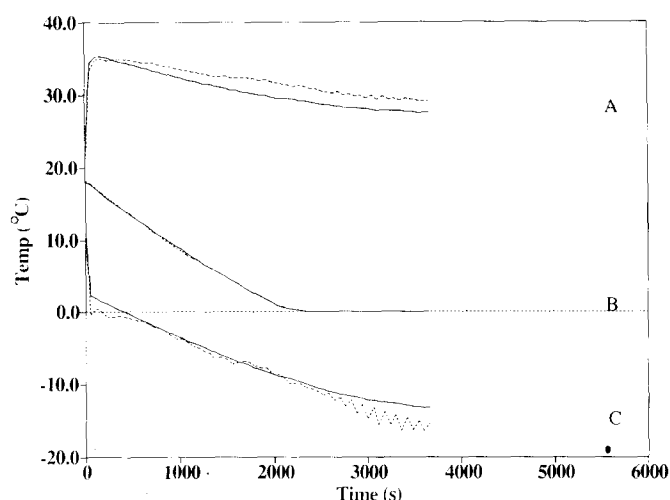


**Figure 3** Plot of measured (----) and predicted (—) temperature ( $^{\circ}\text{C}$ ) versus time (s) during Run 1. (A) Saturated discharge temperature; (B) water temperature; and (C) saturated suction temperature. Figure 3 Tracé des températures ( $^{\circ}\text{C}$ ) mesurées (----) et prévues (—) par rapport à la durée au cours du fonctionnement 1. (A) température de refoulement saturée; (B) température de l'eau; et (C) température d'aspiration saturée

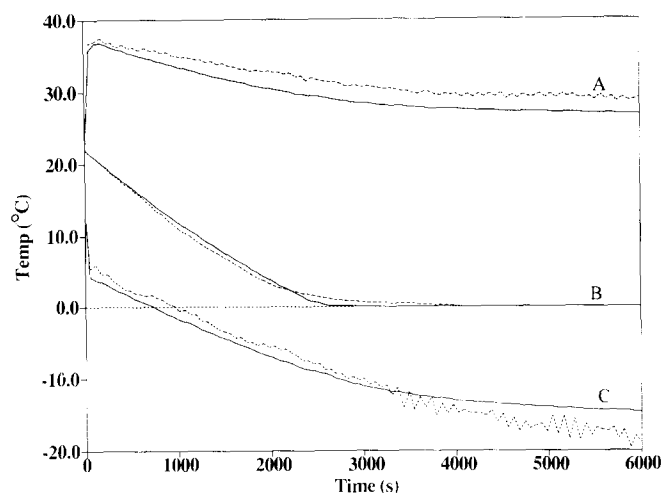


**Figure 5** Plot of measured (----) and predicted (—) temperature ( $^{\circ}\text{C}$ ) versus time (s) during Run 3. (A) Saturated discharge temperature; (B) water temperature; and (C) saturated suction temperature. Figure 5 Tracé des températures ( $^{\circ}\text{C}$ ) mesurées (----) et prévues (—) par rapport à la durée au cours du fonctionnement 3. (A) température de refoulement saturée; (B) température de l'eau; et (C) température d'aspiration saturée

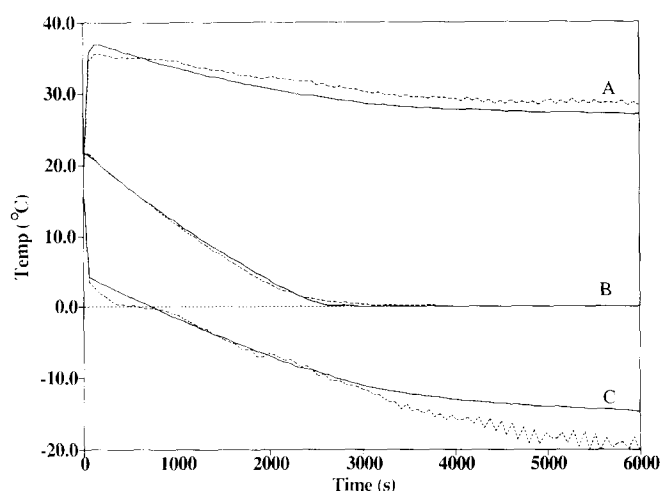


**Figure 4** Plot of measured (----) and predicted (—) temperature ( $^{\circ}\text{C}$ ) versus time (s) during Run 2. (A) Saturated discharge temperature; (B) water temperature; and (C) saturated suction temperature. Figure 4 Tracé des températures ( $^{\circ}\text{C}$ ) mesurées (----) et prévues (—) par rapport à la durée au cours du fonctionnement 2. (A) température de refoulement saturée; (B) température de l'eau; et (C) température d'aspiration saturée

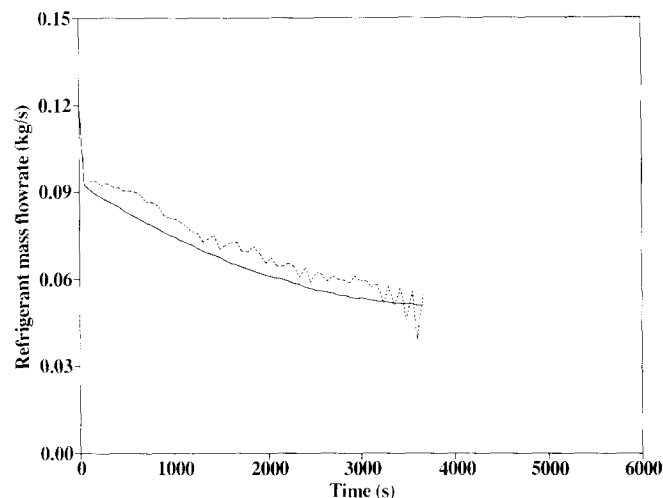


**Figure 6** Plot of measured (----) and predicted (—) refrigerant mass flowrate ( $\text{kg s}^{-1}$ ) versus time (s) during Run 1. Figure 6 Tracé du débit masse du frigorigène ( $\text{kg s}^{-1}$ ) mesuré (----) et prévu (—) par rapport à la durée au cours du fonctionnement 1

areas of the coil in which the relativity of the local convection heat transfer coefficients in the water, and in the refrigerant changed significantly (e.g. parts of the tube partly sheltered from the action of the impeller, areas with high or low boiling activity in the refrigerant). There is also a small pressure drop in the evaporator tubes which would lower the evaporation temperature as refrigerant moves through the circuit. The result is that ice formation probably started earlier than predicted on some parts of the coils. Another possible reason is inaccuracy in  $\alpha_1$  and  $\alpha_3$  (which are mean heat transfer coefficients for the system as a whole). If  $\alpha_1$  is increased and  $\alpha_3$  changed in such a manner that  $(UA)_e$  is held constant the shape and slopes of the predicted lines on Figures 9, 10

and 11 are not significantly altered, but the lines as a whole move left. Overall, considering the simplicity of the model for representing a complex heat transfer situation it was concluded that agreement was probably satisfactory. The rate of ice formation (defined by the slope of the ice formation graphs) was better predicted than the time ice formation started.

Turning now to Figures 3, 4 and 5, it can be seen that water temperature is well predicted. Saturated suction temperature is well predicted other than at the beginning and end of each run. The relatively poor prediction at short times was expected from the earlier work of Darrow *et al.*<sup>2</sup>, because the model takes no account of start-up effects. The poor prediction at long times has two causes. The first is that at times after 5000 s the model is no longer valid due to the problem of intersection of ice

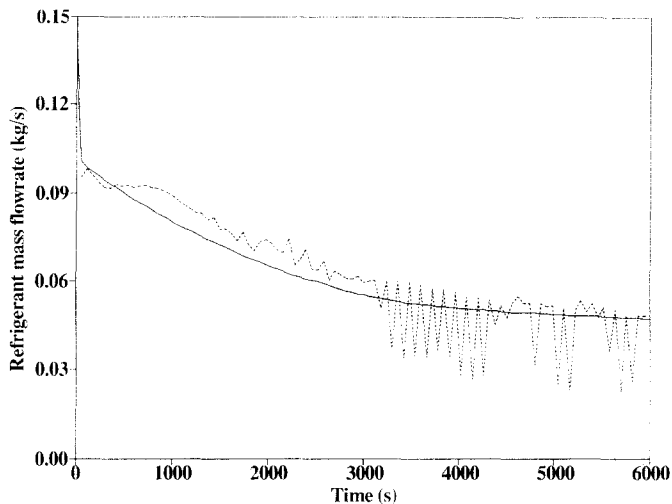


**Figure 7** Plot of measured (---) and predicted (—) refrigerant mass flow rate ( $\text{kg s}^{-1}$ ) versus time (s) during Run 2.  
Figure 7 Tracé du débit masse du frigorigène ( $\text{kg s}^{-1}$ ) mesuré (---) et prévu (—) par rapport à la durée au cours du fonctionnement 2

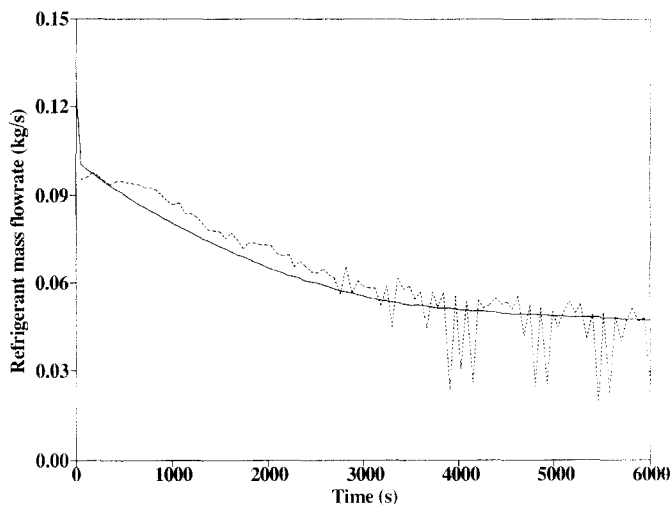


**Figure 8** Plot of measured (---) and predicted (—) refrigerant mass flow rate ( $\text{kg s}^{-1}$ ) versus time (s) during Run 3.  
Figure 8 Tracé du débit masse du frigorigène ( $\text{kg s}^{-1}$ ) mesuré (---) et prévu (—) par rapport à la durée au cours du fonctionnement 3

fronts, as discussed above. The second is that as the saturated suction temperature drops the thermostatic expansion valve is progressively detuning, and eventually its performance loses stability. At this point the assumption that the expansion valve maintains a constant degree of wetting of the evaporator starts to break down, and the predicted and measured lines start to diverge. This happens at a saturated suction temperature just below  $-10^{\circ}\text{C}$ , and is most clearly seen in Figure 3 for Run 1.

On Figures 3, 4 and 5 the results for saturated discharge temperature show a consistent trend of the predicted line being below the measured line except at short times. Sensitivity analysis showed that better prediction could be obtained by lowering  $(UA)_c$ . In the present work  $(UA)_c$  had not been re-estimated, but rather the data of Darrow *et al.*<sup>2</sup> had been used. One possible reason for the real  $(UA)_c$  being lower than that measured by Darrow *et*

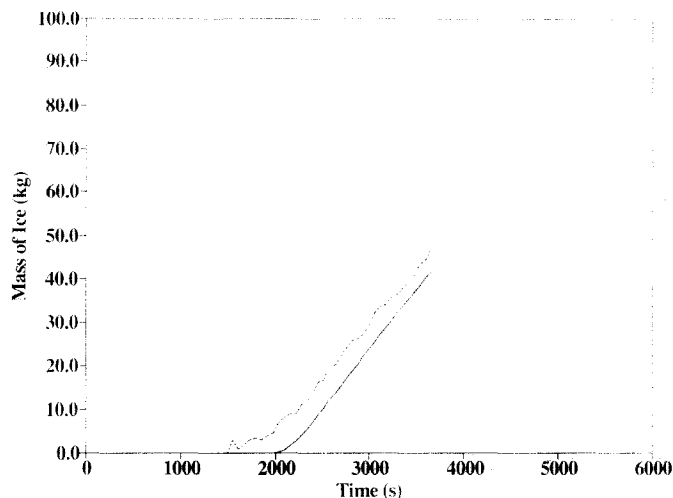


**Figure 9** Plot of measured (---) and predicted (—) ice mass (kg) versus time (s) during Run 1.  
Figure 9 Tracé de la masse de glace (kg) mesurée (---) et prévue (—) par rapport à la durée au cours du fonctionnement 1

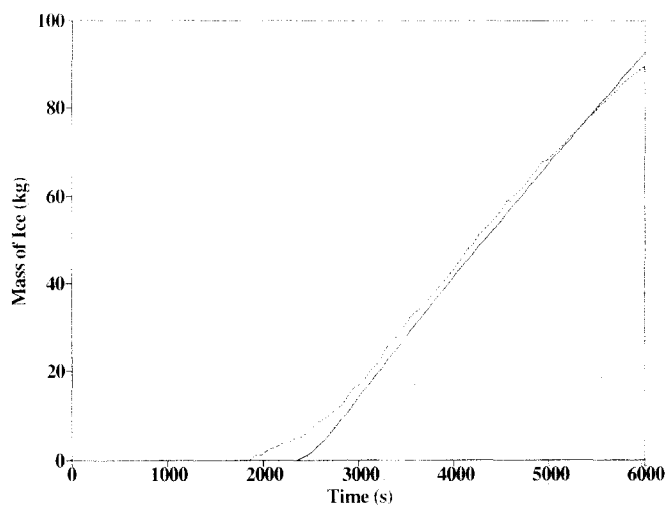


**Figure 10** Plot of measured (---) and predicted (—) ice mass (kg) versus time (s) during Run 2.  
Figure 10 Tracé de la masse de glace (kg) mesurée (---) et prévue (—) par rapport à la durée au cours du fonctionnement 2

*al.* was that the water side of the condenser had not been cleaned, and in the interval of about one year between the two studies some fouling may have built up. However, the more likely explanation related to refrigerant charge. The plant had a combined condenser/receiver, and so if there was any excess of charge this would sit in the bottom of the heat exchanger, covering some of the heat transfer surface, and thus effectively lowering  $(UA)_c$ . Early in the run the amount of refrigerant in the condenser/receiver would be expected to be at its minimum, and later, as vapour specific volumes in the low pressure part of the system rose due to dropping suction pressure the liquid level in the condenser/receiver would build up, thus lowering  $(UA)_c$ . This explanation is consistent with the observed behaviour. The varying extent of the offset between predicted and measured data for the three runs may relate to differing liquid charges, as discussed earlier.

A further possibility for explaining poor agreement

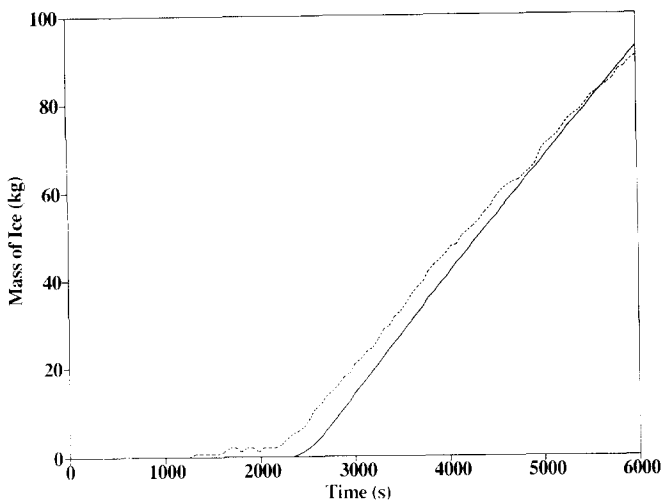


**Figure 11** Plot of measured (---) and predicted (—) ice mass (kg) versus time (s) during Run 3.

Figure 11 Tracé de la masse de glace (kg) mesurée (---) et prévue (—) par rapport à la durée au cours du fonctionnement 3

between measured and predicted saturated suction and discharge temperatures was error in the pressure drop allowances which would tend to lead to systematic differences between experiment and prediction. The shape of the plots suggests that this was not a likely cause of error for the saturated suction temperature results. For the saturated discharge temperature the error in the pressure drop allowance would have to be very large (more than 50%) to explain the total difference, and this was considered unlikely. However, error in pressure drop may be a contributor to the offset.

Figures 6, 7 and 8 show the refrigerant mass flow rate data. Two major effects are visible – the inconsistent results once the thermostatic expansion valve started to de-tune, and a consistent offset between the predicted and measured data. Weaknesses in assumptions made in deriving the model, e.g. any error in the assumption of zero liquid subcooling in refrigerant leaving the condenser, would be expected to affect the refrigerant mass flow rate results to some extent, but error in flow meter calibration was thought to be a major contributor. Funds were not available to have the meter independently recalibrated by a reliable test laboratory so this could not be verified.

In the theory section two possibilities for improving the model by replacing  $\Delta h_{fw}$  with terms including allowance for sensible heat effects had been proposed. In the light of the results which showed that the lack of fit seemed to lie in other areas, these proposals were not implemented.

## Discussion and conclusions

During the analysis of the results a number of changes that would have improved agreement between measured and predicted results were identified. In almost all cases these would have involved moving to much more complicated models (e.g. modelling liquid volume in the condenser/receiver to take account of the effect of refrigerant present on  $(UA)_c$ , modelling the dynamics of the expansion valve, modelling non-cylindrical ice growth). These were not implemented as they did not meet the objectives of the work, i.e. to find out how well a simple model that

did not take account of hydrodynamic and complex heat transfer effects would perform. The results show that the conclusions of Darrow *et al.*<sup>2</sup> for operating the plant as a water chiller are also applicable to its operation as an ice bank. It is valid to model the plant using a model based on 'thermal analysis' provided the inherent shortcomings of thermal models are recognized. One would expect that if the plant had been equipped with separate condenser and receiver, and with an expansion valve that continued to operate satisfactorily across the full range of conditions encountered, deviations from the modelled behaviour would have been smaller. Thus this work provides further evidence that thermal models can be adequate, but that it is important that their limitations are clearly recognized.

The second objective of the work was to ascertain whether the model proposed would be suitable for use in ice-bank design. There are two requirements for suitability – can the data required to use the model be found, and is its prediction accuracy likely to be adequate in practice? With respect to the latter requirement, one concern is that after ice growth from two adjacent tubes has intersected, any subsequent melt-back may not take the ice front shape back to separate cylinders because the temperature profile within the ice would be modified. This was not pursued because loss of surface area significantly affects ice formation rate, and so a system designer would want to avoid such a situation. Whilst the time that ice formation started was not accurately modelled, the rate of ice formation was well predicted. The error is probably tolerable for many design situations.

To use the model in design there are few data which the model needs that the designer would not need to know to carry out an effective steady state design. The performance of the compressor (as expressed in its isentropic and volumetric efficiencies) must be known. Pipeline pressure drop would always be worked out at at least one condition, and these data can be extended to other conditions by using the proportionality relationship applied in this work. The heat transfer coefficients in the condenser and evaporator must also be known for the design, as must the physical measurements of the plant. There may be some difficulty in obtaining data for  $(Mc)_c$  and  $(Mc)_e$ . Darrow *et al.*<sup>2</sup> showed that the results were not particularly sensitive to uncertainty in these parameters. They used estimates based on the mass of metal in the heat exchanger, plus an allowance for the amount of refrigerant expected to be in the exchanger. If the total expected refrigerant charge is known then an arbitrary assumption that perhaps 30–50% is in each of the condenser and evaporator may be adequate.

The last two requirements to use the model are a numerical integration package, and thermodynamic data for the refrigerant. The ODEs are not complex, and can be handled by well-known numerical integration methods such as the fourth order Runge–Kutta method. The curve-fit thermodynamic data routines of Cleland<sup>5</sup> are relatively simple to incorporate in the model. The net result is that a simple computer program that will run on a low level personal computer will perform the calculations.

In the use of the model for design the external heat load on the system is added into the right hand side of Equations (3) and (12). This load can be made to vary with time in any fashion. Useful outputs from the model



would be instantaneous COP, mass of ice present, compressor energy use, etc.

Although it will not give accurate predictions at all times during a simulation, and for all sets of possible operating conditions, the simple dynamic model is suitable for use in many situations by ice bank designers, and the data requirements to use it are not excessive.

## References

- 1 Cleland, A. C. *Food Refrigeration Processes: Analysis, Design and Simulation* Elsevier Science Publishers, London (1990)
- 2 Darrow, J. B., Lovatt, S. J., Cleland, A. C. Assessment of a simple mathematical model for predicting the transient behaviour of a refrigerant system *Proc 18th Int Congr Refrig* (1991) 1189-1192
- 3 James, K. A., James, R. W., Dunn, A. *A critical survey of dynamic models of refrigeration systems and heat pumps and their components* Technical Memorandum No. 97, Institute of Environmental Engineering, Polytechnic of the South Bank, London (1990)
- 4 Plank, R. Die gefrierdauer von eisblocken *Zeitschrift für die gesamte Kälte-Industrie* (1913) **20**(6) 109-114
- 5 Cleland, A. C. Computer subroutines for rapid evaluation of refrigerant thermodynamic properties *Int J Refrig* (1986) **9** 346-351